

METHODOLOGY ARTICLE

Open Access



Micro-CT imaging of live insects using carbon dioxide gas-induced hypoxia as anesthetic with minimal impact on certain subsequent life history traits

Danny Poinapen^{1,3*†}, Joanna K. Konopka^{2,3†}, Joseph U. Umoh¹, Chris J. D. Norley¹, Jeremy N. McNeil² and David W. Holdsworth¹

Abstract

Background: Live imaging of whole invertebrates can be accomplished with X-ray micro-computed tomography (micro-CT) at 10-100 μm spatial resolution. However, image quality could be compromised by the movement of live subjects, producing image artefacts. We tested the feasibility of using CO_2 gas to induce temporary full-immobilization of sufficient duration to image live insects based on their ability to tolerate hypoxic conditions. Additionally, we investigated the effects of these prolonged hypoxic conditions on several life history traits of a lepidopteran species.

Methods: Live Colorado potato beetle (CPB) and true armyworm (TAW) adults were immobilized under a constant CO_2 gas flow (0.5 L/min), and scanned using micro-CT (80 kVp; 450 μA). An $\text{L}_8 (2^4)$ orthogonal array (OA) was used to evaluate the effects of prolonged CO_2 -induced anesthesia on the recovery, longevity, and incidence of mating of TAW adults. The variable factors were age (immature and mature), sex (female and male), exposure time (3 and 7 h), and exposure regime (single and repeated).

Results: With this method, successful 3D reconstruction and visualizations of CPB and TAW adults were produced at 20 micron voxel spacing at an acceptable radiation dose and image noise level. From the inverse-square relationship found between the radiation doses and image noise levels, the optimal scanning protocol produced an entrance dose of 6.2 ± 0.04 Gy with images of 129.6 ± 5.1 HU noise level during a 2.7 h scan. Independent OA experiments indicated that CO_2 gas did not result in death of exposed TAW adults, except when older males were exposed for longer durations. Exposure time and sex were more influential factors affecting recovery, longevity, and mating success than age and exposure regime following CO_2 exposure.

Conclusion: We have demonstrated that using CO_2 gas during micro-CT imaging effectively induces safe, repeatable, whole-body, and temporary immobilization of live insects for 3D visualizations without motion artefacts. Moreover, we have shown that exposed TAW individuals made a full recovery with very little impact on subsequent longevity, and mating success post hypoxia. This method is applicable to other imaging modalities and could be used for routine exploratory and time-course studies, for repeated scanning of live and intact individuals.

Keywords: Live insect imaging, Hypoxia, Anesthesia, X-ray micro-computed tomography, Orthogonal array design, Recovery, Longevity, Mating success, *Leptinotarsa decemlineata*, *Pseudaletia unipuncta*

* Correspondence: dpoinapen@robarts.ca; dpoinapen@gmail.com

†Equal contributors

¹Preclinical Imaging Research Centre, Robarts Research Institute, Schulich School of Medicine and Dentistry, Western University, London, ON, Canada

³London Research and Development Centre, Agriculture and Agri-Food Canada, London, ON, Canada

Full list of author information is available at the end of the article



Background

Conventional imaging methods, such as light and confocal microscopy, provide valuable details of internal anatomy of invertebrates, but they generally require sacrifice or dissection of the live individuals [1]. The use of these methods in longitudinal (time-course) studies, involving repeated scans of the same individuals, is thus not possible. Magnetic resonance imaging (MRI), and X-ray micro-computed tomography (micro-CT) [2, 3] have been used for 3D non-destructive visualization of internal anatomical structures [4–10] of live and preserved small mammals and invertebrates, including insects [11–20]. Micro-CT and MRI each have their own advantages and limitations due to organism size (scanner field of view), spatial resolution, scan time and cost. While these two techniques have produced reasonably high-resolution images of both dead and live insects [5, 10, 21, 22], difficulties were encountered due to internal and external body movements, and required physical restriction of the individuals. Such physical constraints induce stress that can affect the behavior and/or physiology of test organisms during and after the imaging procedure.

Insects can tolerate high doses of ionizing radiation, as during micro-CT, due to highly efficient oxidative stress and DNA damage repair mechanisms [23–26]. Some lepidopteran cell lines are reported to tolerate X-ray doses 52–104 times more than mammalian counterparts [23, 24]. Nevertheless, death or permanent metabolic damage due to radiation has been observed, especially when synchrotron beams are employed (> 300 Gy) [6, 9]. These high radiation doses preclude the possibility of repeated measures on the same living individuals over time, and therefore keeping the radiation doses as low as possible becomes crucial to avoid rapid death during follow-up studies on live insects using micro-CT.

Therefore, an ideal imaging protocol for studying live insects would preferably accommodate the following criteria: allow simultaneous scanning of multiple, fully-intact specimens to maximize throughput; provide adequate image resolution and high contrast-to-noise ratio to distinguish *in situ* structures; deliver a sufficiently low radiation dose to allow repeated scans for time-course studies; and allow fully-immobilized individuals to eliminate motion-related artefacts. Additionally, the protocol should have minimal or no subsequent negative effects on the life history traits or physiological processes of test subjects.

To minimize motion artefacts during live insect X-ray micro-CT imaging, we temporarily immobilized the test subjects using hypoxia by carbon dioxide (CO₂) gas. In addition to being radiotolerant, insects can survive acute hypoxic (oxygen deficient) conditions [27–29]. Keeping insects in CO₂ hypoxic and /or hypercapnic (abnormally elevated CO₂ level) conditions leads to temporary, whole-body

immobilization as the CO₂ molecules mainly interfere with the neuromuscular junction (NMJ), probably by blocking the glutamate receptors [27–29]. In this state, CO₂ induces anesthesia that stops both external (e.g. antennae and legs) and internal (e.g. heart beat and hemolymph flow) body movements [17, 30], thereby eliminating motion-related image artefacts.

Since live insect scanning typically takes at least several hours to complete when using bench-top micro-CT, prolonged exposure to either ionizing radiation or CO₂ gas could negatively affect aspects of insect behaviour and fitness [31–35]. Such exposures could be detrimental in time-course studies where the same individuals must be examined multiple times. Thus, an optimized imaging protocol should ensure safe entrance doses, preferably at least 10 times less than commonly used during insect sterilization. The effects of prolonged exposure to hypoxic conditions can be long lasting, and may not necessarily be immediate. Therefore, it is critical to distinguish between possible effects of experimental treatments and those of hypoxia-induced anesthesia. Several factors including age, sex, duration of acute exposure, and number of repeated exposures play a role in insects' response to and recovery from hypoxia. Their relative importance may vary depending on the subsequent effects on life history traits, and consequently on the type of biologically-relevant processes under investigation. Therefore, in parallel to investigating the feasibility of using CO₂ gas for immobilization of live insect (the Colorado potato beetle and the true armyworm) adults undergoing micro-CT scanning, we assessed the effects of prolonged CO₂ exposure, of equivalent duration required for imaging experiments on the recovery, longevity, and mating of *Pseudaletia unipuncta* adults. To this end, we employed an orthogonal array design – a robust and unbiased method to determine the influence of individual factors, while limiting experimental variability [36–40]. This approach yields the optimized combinations of factors that have a minimal impact on the recovery and certain subsequent life history traits of insects post-anesthesia during live imaging.

Methods

Insects

Colorado potato beetle (CPB; *Leptinotarsa decemlineata* Say, Coleoptera: Chrysomelidae) and the true armyworm (TAW; *Pseudaletia unipuncta* Haworth, Lepidoptera: Noctuidae) were obtained as newly-emerged adults from laboratory colonies maintained at Agriculture and Agri-Food Canada and the University of Western Ontario, respectively. Appropriate food sources were provided for each species: potato leaves for the CPB, and ad lib 8% (w/v) sugar water solution for the TAW.

Anesthesia, scanning, and data acquisition

Immediately before micro-CT imaging, the live adults were immobilized (~10-20 s) under a constant flow (5 psi; 0.5 L/min flow rate) [41] of medical grade carbon dioxide (CO₂), and placed in a custom designed tube (Fig. 1a) for micro-CT scanning. This tube was made with the conical end of a 50 mL centrifuge tube cutoff. A plastic syringe filter was affixed to the open end to which a Tygon tube (R-3603; I.D. × O.D. 1/4 in. × 3/8 in) was connected for CO₂ gas delivery. A rectangular piece of radiolucent expanded polystyrene foam was used as a bed to support the anesthetized insects. Two moistened foam pieces were interposed at either end of the tube to prevent insect desiccation. The insects were kept under anesthesia for a further 10 min to ensure full immobilization before scanning, after which the flow of CO₂ gas was continued for the full duration of each scan.

The tube containing the live individuals was scanned in a GE eXplore Locus RS-9 X-ray micro-CT system (GE Healthcare, London, Canada). The acquisition parameters for the various scan protocols are detailed in Table 1. X-ray projections were acquired over a full 360° rotation around the sample volume (except for Protocol 1 acquired over a 191° rotation; Table 1).

One week-old CPB adults (2 males and 2 females), including a water sample for Hounsfield Units (HU)

calibration, were scanned (field of view = 3.8 × 3.8 × 3.8 cm; see Additional file 1: Figure S1(I)) using Protocols 1, 2, and 3 (see Table 1). The insects were then allowed to recover for 48 h, before being scanned using Protocol 4. Finally, after a further 24-48 h recovery, these CPB were scanned using Protocol 5. The 24-48 h recovery periods were to ensure full restoration of normal metabolism between scans [42]. Although the CPB females recovered after being scanned using Protocol 4, they died within 48 h, and were replaced by two new females of the same generation and age for scanning using Protocol 5. The use of these 5 protocols enabled dose and image noise measurements from which the optimal scan parameters were deduced. This optimized protocol was then used to scan TAW adults (2 males and 2 females per scan, including a water sample for HU calibration) when they were 1-d old (sexually immature) and 4-d old (sexually mature).

For both species, during each scanning protocol, the same number of individuals was set aside with no CO₂ exposure and no food for longevity comparison with the scanned ones. For reproducibility, we performed the scanning experiments twice on two fresh batches of CPB (*n* = 4 females; *n* = 4 males; 2 individuals of each sex per scan) and four times TAW (*n* = 4 males; *n* = 4 females; 1 individual of each sex per scan) independently.

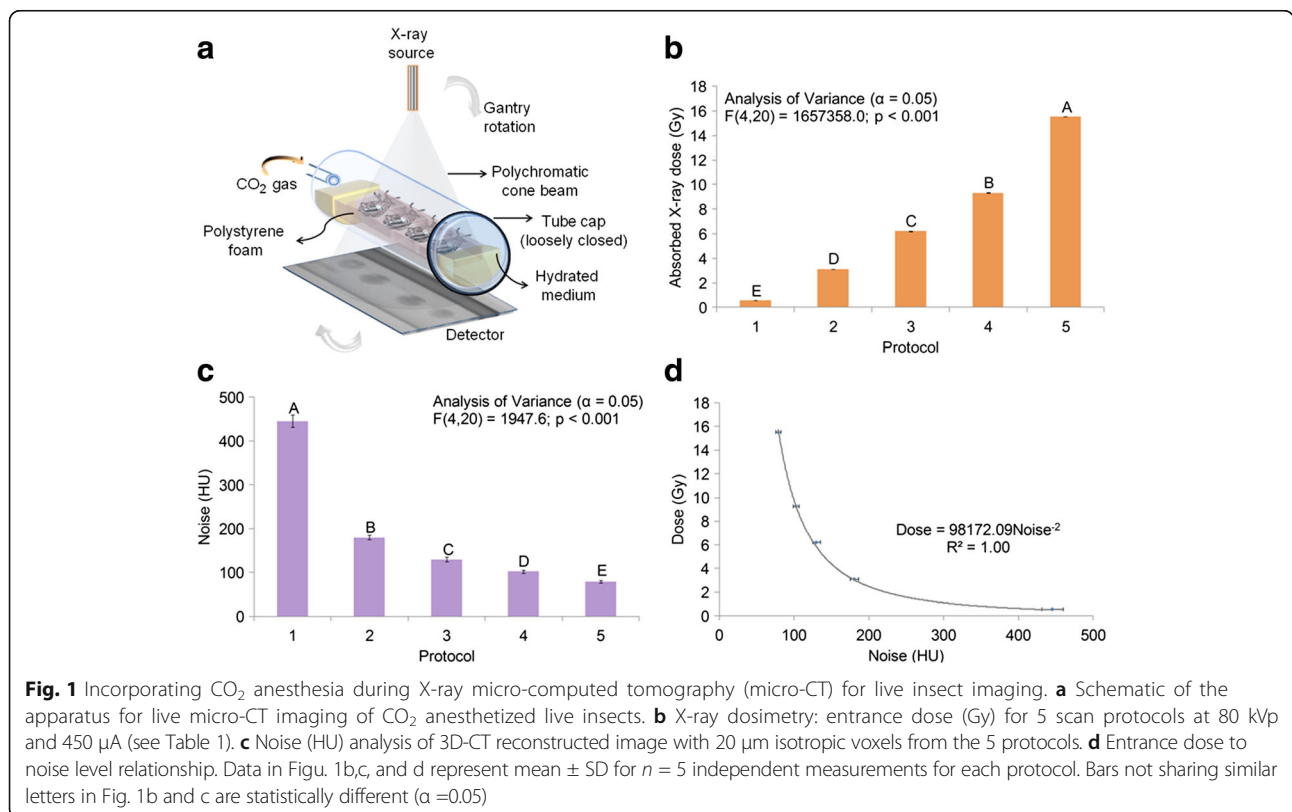


Table 1 Protocol parameters used for scanning live anesthetized adult insects

Protocol (80 kVp; 450 μ A)	Views	Frames per view	Exposure (mAs)	Scan time (h)
1	191	2	343.8	0.33
2	900	1	1822.5	1.40
3	900	2	3645.0	2.68
4	900	3	5467.5	3.96
5	900	5	9112.5	6.53

Dosimetry and noise analysis

The entrance dose (Gy) for the 5 different scan protocols, of duration 0.33, 1.40, 2.68, 3.96, and 6.53 h, was measured at the isocenter of the micro-CT scanner, using an ionization chamber coupled to an electrometer (Keithley, models 96035B and 35614, respectively; see Additional file 1: Figure S1(II)). For each protocol, the noise level (HU) in 3D-CT reconstructed images at 20 μ m isotropic voxel spacing was calculated as the standard deviation of 5 specific regions of interest (ROI) of size 20 \times 20 \times 20 voxels each in a water phantom image volume. The optimal scanning protocol—the shortest scan time that provides the most satisfactory image quality in terms of entrance dose and image noise—was then established from a dose-noise relationship by plotting the entrance dose (Gy) versus noise (HU) [43].

Reconstruction and 3D image rendering

The acquired 2D projections were reconstructed at 20 μ m isotropic voxel size into a 3D image using the Feldkamp filtered-back projection algorithm (FDK) [44] using the GE Healthcare eXplore Reconstruction Utility. The 3D-CT images (in .vff format) were imported as DICOM in Osirix (v. 4.0 32-bit; Pixmeo; GE; Switzerland; freely available at: <http://www.osirix-viewer.com>) for renderings. No manipulations, such as noise averaging, were made to the data. The settings for the 3D MPR (multi-planar reformatted) were: Opacity = linear table, Mode = Volume Rendering (4.03 mm); and for 3D volume rendering (Group: Soft Tissue CT, preset 6 (Soft + Skin), Level of Detail (Fine); Shading (Ambient Coeff. = 0.14; Diffuse Coeff. 0.83; Specular Coeff: 0.50; Specular Power = 50.0).

Orthogonal array (OA) design and setup for CO₂ exposure

To evaluate the effects of prolonged CO₂-induced anesthesia on the recovery, longevity, and incidence of mating, we exposed TAW adults to several treatments based on an L₈ (2⁴) (four factors at two levels) orthogonal array (OA). In this design (Tables 2 and 3; *n* = 10 per treatment), the factors were: age (immature and mature), sex (female and male), exposure time (3 and 7 h—equivalent to micro-CT scan durations), and exposure regime (single and repeated) to a constant flow of

Table 2 Four factors at two levels used in orthogonal array design

Levels	Factors			
	Age (d)	Sex	Exposure time (h)	Exposure regime
1	Immature (IM)	Female (F)	3	Single (S)
2	Mature (MAT)	Male (M)	7	Repeated (R)

CO₂ (5 psi; flow rate 0.5 L/min; see Additional file 1: Figure S2) during the photophase.

We performed this study on TAW adults only because of availability and shorter life span compared to CPB (> 30 d). The controls received no anaesthesia and were not provided with any food source during the periods that treated individuals were exposed to CO₂. All insects, treated and controls, were held in individual clear plastic cylinders with ad lib food source (cotton wicks soaked in 8% sugar water solution) before and after all treatments (Table 3). For repeated anesthesia, the individuals were exposed to CO₂ for a second time 24 h after the first exposure.

For the CO₂ exposure set up, the TAW adults were knocked out for 10–20 s, and carefully placed in a 1 L glass beaker on a layer of polystyrene foam. The beaker also contained a moistened foam support to prevent insect desiccation (see Additional file 2: Figure S2). A funnel was then connected to the chamber for CO₂ gas delivery (medical grade; 5 psi; 0.5 L/min), and the individuals were maintained under these conditions for the required durations according to Table 3. All exposures were performed at 23 °C in light conditions (corresponding to the photophase that insects were entrained to).

Recovery, longevity, and incidence of mating

Post-anesthetic recovery of TAW adults was recorded for each individual as vitality signs (elapsed time for antennae, proboscis, and leg movements), and recovery (flip, walk, and move in a coordinated fashion) time.

Table 3 L₈ (2⁴) matrix (four factors at two levels) showing the treatments from the OA design

Treatments	Factors			
	Age (d)	Sex	Exposure time (h)	Exposure regime
1	IM	F	3	S
2	IM	F	7	R
3	IM	M	3	R
4	IM	M	7	S
5	MAT	F	3	R
6	MAT	F	7	S
7	MAT	M	3	S
8	MAT	M	7	R

Note: Age: IM = sexually immature (1d) and MAT = sexually mature (4d); Sex: F = female and M = male; Exposure time 3 and 7 h correspond to scanning duration for micro-CT protocols; and Exposure regime: S = single (3 or 7 h); R = repeated (3 + 3 or 7 + 7 h)

Longevity of all anesthetized virgin individuals was also recorded and compared with control individuals of the same sex. Virgin individuals were chosen to avoid possible reduction in longevity due to mating. A total of 80 individuals (10 per treatment) were anesthetised, with an equal number of controls (80 total; 10 per corresponding treatment), and used for measurements of recovery and longevity.

To investigate the effects of anesthesia on the incidence of mating, 24 h post-exposure, CO₂-exposed males and females (including control individuals) were paired up with one non-anesthetised virgin mature individual of the opposite sex for the duration of one scotophase (8 h). This pairing ensured that any observed effects on the incidence of mating were due to the exposed individuals. Mating pairs were placed in small mesh cages (22 × 15 × 15 cm) containing ad lib sugar water solution. After 8 h, the respective females of each treatment were dissected to determine if mating was successful by looking for presence of a spermatophore. A total of 80 (in addition to the 80 individuals used for recovery and longevity measurements) individuals (10 per treatment) were anesthetised and paired with non-exposed virgin counterparts for mating experiments. An equal number of non-exposed individuals was used as control and paired with virgin counterparts.

Data analysis

All data were verified for normality using the Shapiro-Wilk's test. Parametric tests (one-way ANOVA followed by Tukey's HSD post hoc test) were used to analyse those data that followed a normal distribution. Otherwise, non-parametric methods (Kruskal-Wallis Test followed by Dunn's test) were employed. The tests and analyses were performed using SPSS (v.21; IBM, NY, USA).

To investigate the effect of a given treatment on the life-span of TAW adults, longevity ratios were computed. For the calculation of this ratio, the mean life span of the female control in each group was calculated and these means were compared using a one-way ANOVA. Since no statistically-significant difference was observed, these data were averaged. This average longevity of the female controls was then used to normalize all the treatments containing females (Treatments 1, 2, 5, and 6). The longevity ratio for females for a given treatment was hence calculated as the average life-span of females from that group divided by the average life-span of all female controls. The average longevity of all male controls was similarly calculated and used to normalize (as they were also not significantly different) treatments containing males (Treatments 3, 4, 7, and 8) to calculate their longevity ratio.

To examine the effect of the treatments on the incidence of mating, each group was compared with its respective control. All female controls were compared to each other; and all male controls were compared to each other using Chi-square tests. Finally, all controls combined (females and males) were compared to each other using a Chi-square test. In all cases no statistically-significant differences were found. Therefore, for the final analysis, a Chi-square test was performed to compare only the mating incidence among the treatments.

The ranking of the impact of the four factors (age, sex, exposure time, and exposure regime) on the outcomes (recovery, longevity, and mating success) based on the L₈ OA [45] was performed in Minitab (v.17 Minitab, Coventry, UK). The reasons for choosing the orthogonal array, rather than a full factorial design, are mainly to reduce the number of experimental treatments and to provide the effective ranking of the factors with respect to their influence on the measured response variables.

After calculating the signal-to-noise (S/N) ratio for each treatment described in Table 3, the average S/N value was computed for each factor and level. This S/N ratio measures the robustness used to establish which of these four control factors (age, sex, exposure time, and exposure regime) result in reduced variability in the outcomes (recovery, longevity, and mating of TAW) by minimizing the impacts of other factors that are not possible to control. These factors, for which we cannot control, are referred as noise, which include genetic variability, individual variation in CO₂ tolerance, gradual increase of lactate level, and acidification during hypoxia. Delta (Δ) was then calculated for each measured parameter (i.e. response) as the difference between the maximum and minimum S/N values. For recovery, the response was computed using eq. (1) below with the goal of minimizing this parameter (smaller the better). Conversely, eq. (2) was used to maximize longevity and mating incidence (larger the better).

$$S/N_i = -10 \log\left(\sum(\bar{y}_i^2)/N_i\right) \quad (1)$$

$$S/N_i = -10 \log\left(\sum(1/\bar{y}_i^2)/N_i\right) \quad (2)$$

where $\bar{y}_i = \frac{1}{N_i} \sum_{u=i}^{N_i} y_{i,u}$ is the mean; i = experiment number, u = trial number and N_i = number of trials for experiment i .

For multivariate analysis, a principal component analysis (PCA) was performed on the recovery, longevity, and mating incidence data. Before performing the PCA analysis, the Kaiser-Meyer-Olkin (KMO; ≥ 0.70 considered as satisfactory to run PCA) measure of sampling adequacy and the Bartlett's test for sphericity (χ^2) were

performed [46]. A PCA using all the measured parameters was then carried out to explore life history trait (recovery, longevity, and mating success) patterns between the 8 treatments post-anesthesia, with varimax rotation after normalization using the z-score on all data in SPSS (v.21; IBM, NY, USA).

Results

X-ray dose-to-image noise relationship

Based on the inverse-square dose-to-noise relationship (Fig. 1d), Protocol 3 emerged as optimal from the dose versus image noise analysis. This protocol resulted in an entrance dose of 6.2 ± 0.04 Gy, producing images (Figs. 2 and 3) with a 129.6 ± 5.1 HU noise level during a 2.68 h scan (i.e. corresponding to the amount of time that the insects were maintained under CO₂ anesthesia). Under these conditions, the insects recovered full mobility within 40 min post-anesthesia/scanning, compared to more than 90 min for the 6.53 h scan (Protocol 5). The 15.5 ± 0.10 Gy entrance dose for the 6.53 h scan was approximately 2.5 times higher than the optimal 2.68 h scan (Fig. 1b), but it was least 13 times less than the average required dose for insect sterilization.

We observed that all CPB individuals (scanned and non-scanned; males and females) lived for approximately 30 d (except for scanned females that did not survive after Protocol 4). No difference was observed in the post-anesthetic longevity of scanned (9.0 ± 2.2 d) and control (10.3 ± 2.9 d) TAW females ($t(6) = -0.70$, $p = 0.51$; $n = 4$; t -test), or between scanned (12.3 ± 1.7 d) and control (11.0 ± 1.4 d) TAW males ($t(6) = 1.13$, $p = 0.30$; $n = 4$, t -test; Fig. 3). Additionally, these TAW adults took

similar time (~ 40 min) to fully recover as those individuals that were exposed to CO₂ for 3 h as shown below.

Post-anesthetic recovery of TAW

Regardless of age and exposure regime, longer exposure to CO₂ gas hypoxia (Treatments 2, 4, 6, and 8) resulted in significantly longer recovery periods in TAW adults of both sexes ($p < 0.0001$; Fig. 4a). Individuals exposed for 7 h took approximately three times as long to fully recover post-anesthesia than those exposed for 3 h. This pattern of longer recovery for individuals with longer exposure times was similar for all other recovery parameters measured, including mean and minimum time to first observed movement, as well as time taken for the insects to flip onto their legs (natural position), and to walk in a coordinated fashion (Additional file 3: Figure S3).

Post-anesthetic longevity of TAW

The observed effect of CO₂ gas hypoxia on longevity of TAW adults was not as pronounced as seen with the recovery parameters. In most cases, exposure to CO₂ gas did not affect longevity of TAW adults. The only exception was Treatment 8, where the males exposed twice for 7 h did not live as long as the controls, or adults exposed for 3 h (Treatments 1, 3, 5, and 7) ($p < 0.01$, Fig. 4b; see Additional file 4: Figure S4a).

Post-anesthetic mating incidence of TAW

Overall, the mating of TAW adults was not affected after exposure to CO₂ gas, except when mature and immature males were exposed once and twice for 7 h (Treatments 4 and 8), where incidence was lower

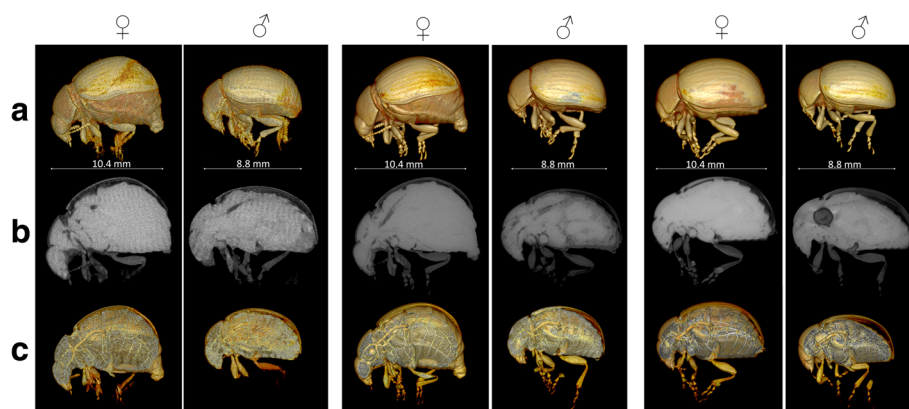


Fig. 2 3D-CT reconstruction of live anesthetized 1 week-old female (♀) and male (♂) Colorado potato beetle adults. Sagittal views of (a) 3D-volume of insect body exoskeleton at 20 μm isotropic voxel spacing; (b) 3D-MPR (multi-planar reformatted) views of the insect body illustrating internal structures; and (c) insect body depicting the tracheal system. These 3D images for Protocol 1 (highest noise; lowest X-ray dose), 3 (optimal), and 5 (lowest noise; highest X-ray dose) allow qualitative comparison of image quality (improving from left to right), noise (decreasing from left to right), and dose (increasing from left to right; see Additional files 7: Videos S1, Additional files 8: Videos S1 and Additional files 9: Videos S2, Additional files 10: Videos S2 for female and male adults, respectively). While the images from Protocol 5 are of the highest quality, the conspicuity of internal structures from the Protocol 3 images are sufficient and spare the individual the higher anesthetic and radiation dose

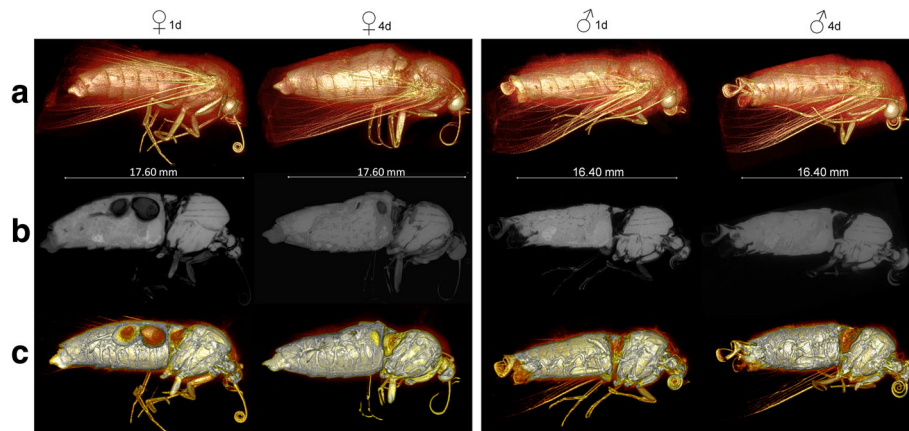


Fig. 3 3D-CT reconstruction of live anesthetized female and male trueyworm adults at 1d and 4d demonstrating the feasibility of repeated scanning of the same individual longitudinally. Sagittal views of **(a)** 3D-volume of the female (♀) and male (♂) body exoskeleton at 20 μm isotropic voxel spacing; **(b)** 3D-MPR (multi-planar reformatted) views of the whole body showing the internal structures; and **(c)** the tracheal system. Protocol 3 was used to image the same individuals at days 1 (sexually immature) and 4 (sexually mature). For renderings of these serial scans, see Additional files 11: Videos S3, Additional files 12: Videos S3 and Additional files 13: Videos S4, Additional files 14: Videos S4 for 1 and 4 d-old female adult, respectively; and Additional files 15: Videos S5, Additional files 16: Videos S5 and Additional files 17: Videos S6, Additional files 18: Videos S6 for 1 and 4 d-old male adults, respectively

compared to all other treatments ($p < 0.05$, Fig. 4c; see Additional file 4: Figure S4b).

Ranking of critical factors

Exposure time was the most influential factor affecting the recovery, longevity, and mating of TAW adults following CO_2 exposure (Table 4). The second most important factors were age and sex of TAW adults. Age influenced only recovery time, but was 10 times less influential than exposure time. Sex impacted longevity ratio, but was 3 times less influential than exposure time. Sex also influenced mating incidence with almost the same influence as exposure time following TAW full recovery. Therefore, the immediate effects of CO_2 anesthesia on the recovery of TAW adults were exposure time- and age-dependent for both males and females. In contrast, long-term physiological effects of CO_2 anesthesia were exposure time- and sex-dependent, as observed for the life history parameters measured many days later.

Additionally, irrespective of the factor rankings, several interactions between different combinations of factors were observed. The recovery time, following CO_2 gas exposure in male and female TAW, was affected differentially depending on the exposure regime (interaction: sex \times exposure regime). Repeated exposures lead to longer recovery times for both sexes. Yet, the difference between recovery time following single and repeated exposures was larger for females than males.

Similarly, longevity of TAW males was negatively affected when sexually mature individuals (4d-old) were subjected to CO_2 (interaction: sex \times age), while no effects were observed with female TAW irrespective of age. The exposure regime had markedly different effect

on longevity of TAW, depending on their age: sexually mature individuals (4d-old) had shorter lives than immature ones (1d-old) after repeated exposure to CO_2 (interaction: age \times exposure regime). Moreover, as exposure time was increased (from 3 to 7 h), there was a greater reduction in longevity of male compared to female TAW (interaction: exposure time \times sex).

Individuals that were sexually mature (4-d old) during CO_2 exposure were less successful at mating after experiencing repeated (interaction: age \times exposure regime) and longer exposure (interaction: age \times exposure time). No effects were observed in any treatment group when sexually immature (1-d old) individuals were exposed to hypoxia. Similarly, the mating success of males was negatively affected when subjected to longer (interaction: sex \times exposure time) and repeated (interaction: sex \times exposure regime) exposures, irrespective of their maturity at the time of exposure to CO_2 .

Multivariate analysis of TAW recovery ability and life-history traits post-anesthesia

Principal component analysis (PCA) with varimax rotation (KMO = 0.7 and $\chi^2(21) = 97.2$; $p < 0.001$) revealed discriminatory patterns among the 8 treatments on the recovery, longevity, and mating of TAW adults post CO_2 -induced hypoxia. The first two principal components (PC1 and PC2) accounted for 95.4% of the total variability (Fig. 5), and separated or grouped some treatments into pairs. Each pair was different from the others (Treatments 1 and 3, 5 and 7, 4 and 8, and 2 and 6) based on their influence on the subsequent recovery and life history traits post-anesthesia (Fig. 5a).

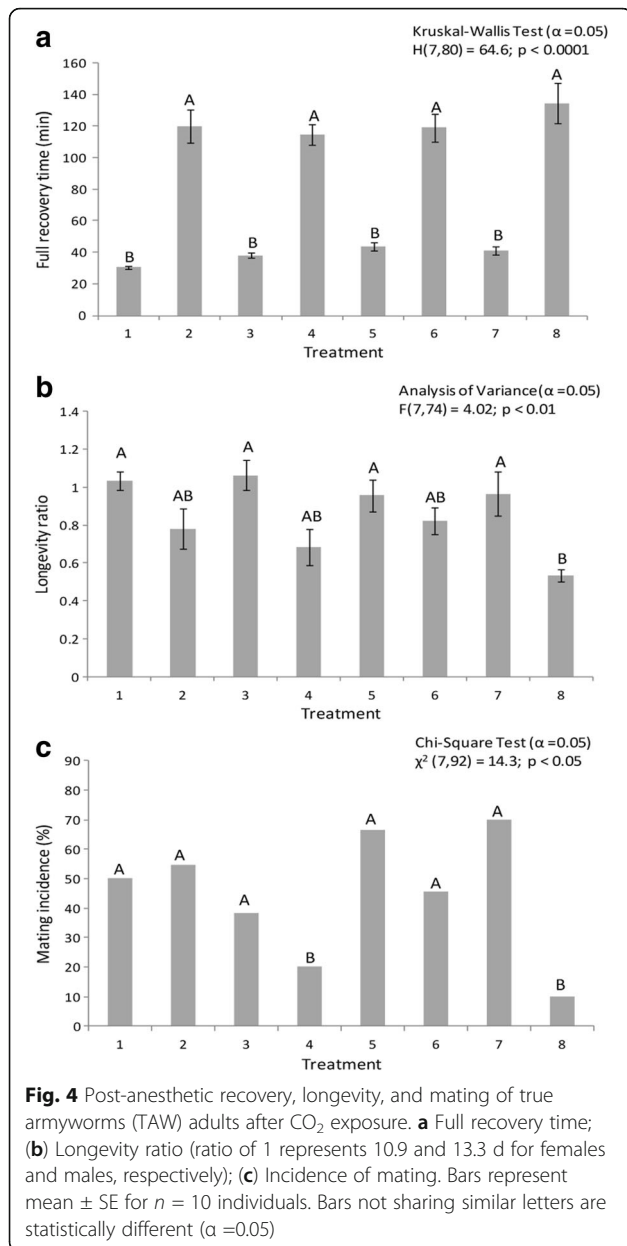


Fig. 4 Post-anesthetic recovery, longevity, and mating of true armyworms (TAW) adults after CO₂ exposure. **a** Full recovery time; **(b)** Longevity ratio (ratio of 1 represents 10.9 and 13.3 d for females and males, respectively); **(c)** Incidence of mating. Bars represent mean \pm SE for $n = 10$ individuals. Bars not sharing similar letters are statistically different ($\alpha = 0.05$)

Principal component 1 (PC1) accounted for 70.5% of the total variability (Fig. 5a), and clearly separated shorter (3 h) exposure time treatments (1, 3, 5 and 7) from longer (7 h) ones (2, 6, 4, and 8). From the PC1 loadings (Fig. 5b), this separation was due to differences

in recovery times post-anesthesia, which is consistent with the statistical analysis of recovery times summarized in Fig. 4a.

Principal component 2 (PC2) accounted for 24.9% of the total variability and separated the treatments based on sex (male vs. female), and age (sexually immature vs. mature) after CO₂ exposure. Examination of PC2 loadings (Fig. 4b) revealed maximum separation was caused mainly by low mating incidence linked to Treatments 4 and 8, which is consistent with the results shown in Fig. 4c. Therefore, any combinations of factors may be used in any TAW imaging study employing CO₂ gas anesthetic, except those of Treatments 4 and 8, namely long exposures for male individuals (Table 3).

Discussion

Our results indicate that incorporating hypoxia and/or hypercapnia to totally immobilize individuals during scanning is a suitable method for visualizing whole live insects using X-ray micro-CT, with little or no impact on their subsequent recovery, longevity and mating success when the optimal conditions are used. Moreover, this method is not only applicable to individuals at adult stage, it has also successfully enabled imaging of live individuals at larval and pupal stages (see Additional file 5: Figure S5). Where inherent tissue contrast is insufficient, non-toxic contrast agents can be further added to the imaging procedure for tissue differentiation enhancement, facilitating segmentation (see Additional file 6: Figure S6). Such contrast agent is not required for rendering and segmenting live insect exoskeleton from soft tissues (fat body and muscles) as reported here and illustrated in Figs. 2c and 3c.

This technique is compatible with various scanning modalities and its ease of implementation is important for its broad application in routine and reproducible scanning. One clear benefit is its application to any lab-based “bench top” scanner for studies using live insects. In spite of synchrotron beamlines being free (pending proposal acceptance) and capable of producing very high-resolution images, longitudinal studies on live insects remain very problematic at these facilities due to logistical reasons (in addition to very high X-rays radiation doses). Even if required regulatory permits are obtained, transportation over long distances can

Table 4 Ranking of factors based on their influence on recovery, longevity, and mating of TAW adults

Parameter	Signal to noise ratio (Δ S/N)			
	Age	Sex	Exposure time	Exposure regime
Recovery	0.97 (2)	0.40 (4)	9.87 (1)	0.90 (3)
Longevity ratio	0.79 (3)	1.17 (2)	3.19 (1)	0.60 (4)
Incidence of mating	0.02 (4)	5.93 (2)	6.29 (1)	1.78 (3)

Δ = difference between the maximum and minimum S/N for each factor at 2 levels. Values represents delta (rank) to 2 decimal places. Factors with a higher Δ value indicate greater influence on the measured parameters. Rank 1 \rightarrow 4 represents highest to least influence

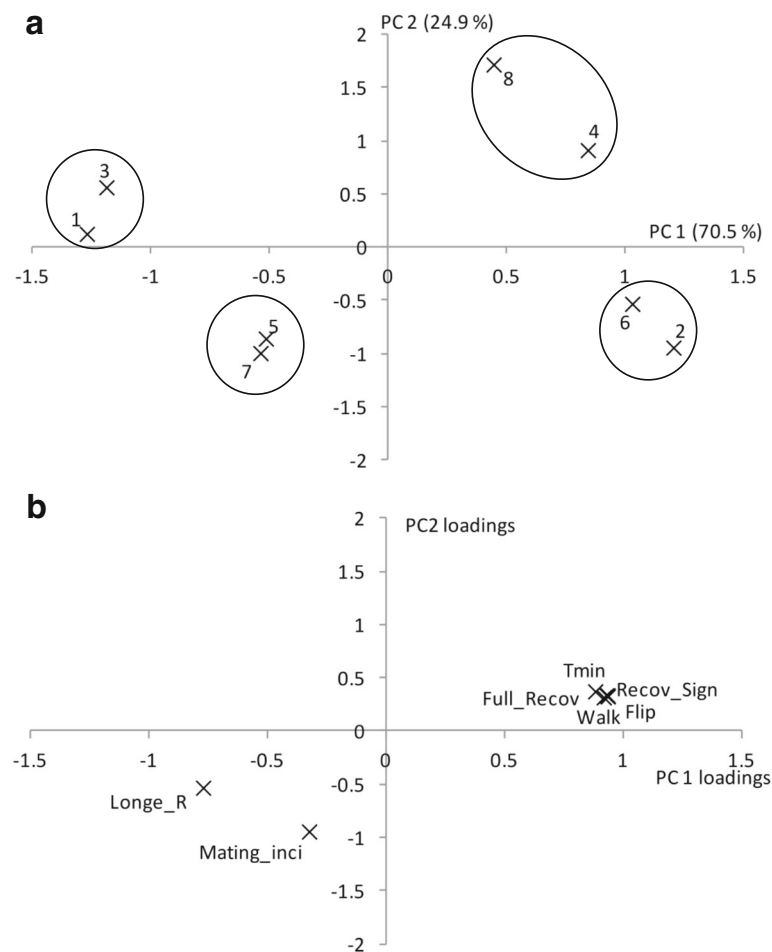


Fig. 5 Principal component analysis (PCA) of TAW adult life history post CO₂ anesthetic exposure. **a** PCA scores plot. Treatments that are grouped together produce similar effects on the recovery, longevity, and mating of true armyworm adults post-anesthesia. **b** PCA loadings plot. The effects of prolonged CO₂ exposure on live insect physiology are temporal, being more prominent at the early stage of recovery. These effects lessen for processes occurring beyond recovery from post-CO₂ in TAW adults. Recov_Sign = vitality sign (min); Tmin = Minimum time for first movement (min); Walk = walking time (min); Flip = Flipping time (min); Full_Recov = Full recovery time (min); Longe_R = Longevity ratio; and Mating_inci = Mating incidence (%)

cause stress to the animals and there is a risk of introduction of invasive species or pest in new areas. These facilities offer little or no adequate rearing space to maintain the specimens used for repeated imaging for time-course studies.

In an imaging context, our findings suggest that hypoxic conditions induced by exposure to CO₂ gas, at least with respect to the investigated critical factors, is not detrimental for the measured life history parameters (longevity and mating) of TAW (except for males exposed for longer durations). Hypoxia and /or hypercapnia induced by CO₂ gas produces reversible loss of motor function in insects (due to lowered sensitivity in neuromuscular junction to glutamate) [28], and can have long-lasting effects on behaviour, including phase shifts in circadian rhythms [47] and life history traits [27]. For example, following CO₂ anesthesia, *Drosophila melanogaster* not only exhibited

reduced longevity, but also lowered fecundity, mating success, and motor function [31, 33, 48]. Similarly, negative effects on development, locomotion, and feeding were observed after CO₂ induced anesthesia in *Blattella germanica* [32, 34]. However, provided that adequate recovery period is allowed, insect physiology following anesthesia usually returns to normal, with recovery proportional to the exposure duration [35, 42, 49], consistent with our findings on the recovery ability in TAW.

The observed reduced longevity and low mating success in TAW males that were exposed to longer durations can be related to body size and age, as seen for those individuals in Treatments 4 and 8. The maximum time that insects can withstand hypoxia is not only species dependent, but within species, females are more tolerant than males because of their larger body size [30, 50], as in the case of the TAW females compared

to males. Larger body size usually indicates larger carbohydrate and fat reserves [51], and possibly allows faster resumption of normal metabolism. Moreover, this hypoxia tolerance declines with age for both sexes [30], which was observed in our study for repeatedly exposed males (compared to single CO₂ exposures).

Regardless of which treatment we employed, the fact that all individuals were able to move their antennae and other appendages post anesthesia suggests no immediate central nervous system (CNS) impairment [30]. During the observed sequence of movement restoration in TAW, starting with extremities and joints followed by coordination of movements and eventual flight, the first two are linked directly to rapid adenosine triphosphate (ATP) re-synthesis [30] once oxygen becomes available again. This rapid ATP re-synthesis results from insects' ability to retain adenylates (products of ATP breakdown) in their tissues – in contrast to mammals. Additionally, because insects accumulate very little lactate during hypoxia exposure [30], they avoid the toxic effects of accumulated metabolic products of glycolysis. Combined together, mobility becomes possible again as coordination of CNS with muscles and metabolism are restored during recovery. This process is independent of the circulatory system because gaseous O₂ flows easily through the tracheae to the brain, and other parts of the CNS, even before circulation is restored. Consequently, CNS dependent processes are preserved, irrespective of whether the organisms live to their full life-span or not, post hypoxia.

The ability to scan multiple individuals in a single scan acquisition, in order to maximize sample throughput, is compromised at higher resolutions, where the field of view is necessarily reduced. In the current study, scanning of multiple organisms simultaneously was possible at 20 μm, which is sufficient to visualize the exoskeleton, its invagination (tracheal system), and larger structures. Nevertheless, scanning of multiple individuals is compromised when higher resolution is needed for resolving very fine structures.

The application of CO₂ anesthesia during micro-CT imaging for visualizing whole live insects is not limited to 20 μm resolution voxel spacing, presented here as a proof of concept. This method is applicable to studies where much higher resolution is achieved [5, 7, 9, 10, 52]. However, at higher resolution, higher radiation doses become more of a concern to the live individuals and moreover, additive effects between prolonged exposure to hypoxic conditions and higher ionizing radiation doses can be expected. In the current study, the scanned individuals received between 13 times (15.5 Gy for Protocol 5) and 345 times (0.58 Gy for Protocol 1) less radiation dose than the average required dose for insect sterilization [24, 53]. This dose was also between 22.5 to 597 times,

and 84 to 2218 times less than that delivered by synchrotron monochromatic (~350 Gy) and polychromatic (~1300 Gy) beams, respectively. Although we cannot definitively rule out the combined effect of X-ray radiation and CO₂-induced hypoxia in our study, we suggest its impact to be minimal because the adult individuals received very low radiation doses during the imaging procedure under prolonged hypoxia exposure. Although the entrance doses were 1 to 2 orders of magnitude less than sterilization dose for adult insects, other life stages such as larval and pupal may have different susceptibility to radiation and CO₂ anesthesia due to the rapid cellular changes that are occurring at these stages. Future comprehensive studies may wish to address this differential impact of radiation on different developmental stages (including adult) in combination with CO₂ anesthesia in a longitudinal study within and across several generations of insects.

Finally, the application of CO₂ gas anesthetic during live imaging can be used to discriminate among different tissues (e.g. muscles, fat body, and alimentary tract) at 20 μm isotropic voxel size to address a number of different questions that would give valuable insights into insect physiology and metabolism. Although we have only investigated the effect of CO₂ anesthesia on adults, this method can be extendable to time-course developmental studies on different stages of development. For example, in studies of migratory moth adults, the technique could provide a non-destructive means of assessing the level of gonad development and lipid accumulation at different times of the year, or determining of mating status (the presence or absence of spermatophores) [54]. Currently, those aspects are invasively determined by dissection. Similarly, the technique could be employed to follow temporal anatomical change during different stages of larval and pupal development in applied entomology. Overall, depending on the measured end point of any experiment on live insects, various combinations of physical scan conditions and biological states of scanned insects become important during imaging as shown by the interactions of factors in our results. There may be other such factors of interest in other investigations, where interactions may exist and are either not obvious, or have subtle effects. To this end, taking full advantage of the OA approach is invaluable in interpretations and understanding of observations that are purely biological, and separated from those due to the imaging procedure. Thus, this method can be expanded to incorporate other factors such as life stages (larval, pupal, and adult) to minimize the impact of using the 6.2 Gy as optimal imaging protocol and CO₂ anesthesia on different life history traits to ensure that longitudinal studies on insect morphology within and beyond several generations are not confounded.

Conclusion

Exposing insects to hypoxic conditions using CO₂ gas, to ensure whole-body unrestricted immobilization, provides a new way to visualize live insects using X-ray micro-CT. 3D images were produced to distinguish in situ structures at 20 μm voxel spacing and at a relatively low radiation dose of less than 20 Gy. Repeated scanning of the same individuals is possible, allowing for time-course studies where live imaging is required. CO₂ anesthesia can be incorporated with many other imaging modalities. Overall, depending on the experimental end points, there exist some combinations of critical factors under which insects can recover fully from hypoxia, without any apparent impact on their longevity and mating success. Since the method is simple to implement, routine time-course studies and other immediate widespread applications can be achieved, wherever live insect visualization is required, in applied entomology, such as medical entomology, insect development, and parasitology, to extract biologically-relevant information.

Additional files

Additional file 1: Figure S1. Set up for micro-CT live insect imaging and dosimetry. (I) Set-up for insect live scan. (A) Specially designed tube placed in a GE eXplore Locus RS-9 scanner containing fully-immobilized individuals by CO₂ anesthesia (5 psi; 0.5 L/min). Anesthetized adults of (B) *L. decemlineata* (CPB) and (C) *P. unipuncta* (TAW). (II) Dosimetry measurement with the isocenter of an ionization chamber placed at insect level. (DOC 776 kb)

Additional file 2: Figure S2. Set up for CO₂ exposure of live insects. Set-up used for exposing live insects to CO₂ gas. Because delivering CO₂ gas at 5 psi (0.5 L/min) for long durations causes formation of ice crystals in the regulator, a 60 W lamp is directly shone on it to prevent frost occurrence. (DOC 845 kb)

Additional file 3: Figure S3. Post-anaesthetic recovery of true armyworms (TAW) adults after CO₂ exposure. (1) Vitality sign (average time taken for proboscis, antenna, and legs movement combined); (2) Minimum time taken for first movement (proboscis or antennae or legs); (3) Flipping time (when the anesthetised moths flip from back-laying (unnatural) to standing positions (natural)); and (4) Walking time (the start of coordinated walk). Bars represent mean ± SE for *n* = 10 individuals. Bars not sharing similar letters are statistically different (α = 0.05). Data that followed a normal distribution were analysed using parametric methods (ANOVA followed by Tukey's HSD test); otherwise, non-parametric methods (Kruskal-Wallis Test followed by Dunn's test) were used. (DOC 653 kb)

Additional file 4: Figure S4. Longevity (a), and mating (b) of CO₂ exposed and control true armyworms (TAW) adults. Bars represent mean ± SE for *n* = 10 individuals. (DOC 448 kb)

Additional file 5: Figure S5. 3D-CT reconstruction of insects at larval and pupal stages. 3D reconstruction at 20 μm isotropic voxels of live anesthetized (I) *P. unipuncta* pupae, and (II) hornworm larva using Protocol 3. (DOC 437 kb)

Additional file 6: Figure S6. Use of non-toxic iodinated contrast agents in live insect micro-CT imaging. 3D reconstruction (at 20 μm isotropic voxels) of live anesthetized females of: (I) 1 week-old *L. decemlineata* (Protocol 5); (II) 1d-old *P. unipuncta* (Protocol 3) showing sagittal views of (a) 3D-volume of exoskeleton; (b) 3D-MPR of whole body showing the internal structures; and (c) the tracheal system. The CPB individuals (I) were allowed to move freely in a plastic Petri dish

containing 20% Lugol's solution (for faster staining) as contrast agent for 1 h. The Petri dish was placed in a slanted position so that the individuals could walk/swim without drowning. These stained insects were able to live and reproduce normally after this staining process and scanning. We did not quantify possible toxicity of this Lugol's solution to the organisms. The TAW adults (II) were fed 8% sugar water containing Omnipaque 350 contrast agent (1:11 w/v; can be adjusted for optimal contrast ratio). (DOC 1929 kb)

Additional file 7: Video S1a. 3D reconstruction of a live 1wk-old anesthetized female CPB adult. Volume rendering of a live 1wk-old anesthetized adult female Colorado potato beetle (*L. decemlineata*) adult showing the exoskeleton, soft tissues, and tracheal system at 20 μm isotropic voxel spacing (micro-CT data acquired using Protocol 3). *Note: The contraction or relaxation of muscles during anesthesia resulted in the ovipositor extrusion.* (MOV 2903 kb)

Additional file 8: Video S1b. 3D reconstruction of a live 1wk-old anesthetized female CPB adult. MPR rendering of a live 1wk-old anesthetized adult female Colorado potato beetle (*L. decemlineata*) demonstrating in situ internal structures arrangements supported by exoskeleton at 20 μm isotropic voxel spacing (micro-CT data acquired using Protocol 3). *Note: The contraction or relaxation of muscles during anesthesia resulted in the ovipositor extrusion.* (MOV 746 kb)

Additional file 9: Video S2a. 3D reconstruction of a live 1wk-old anesthetized male CPB adult. Volume rendering of a live 1wk-old anesthetized adult male Colorado potato beetle (*L. decemlineata*) illustrating the exoskeleton, soft tissues, and tracheal system at 20 μm isotropic voxel spacing (micro-CT data acquired using Protocol 3). (MOV 2308 kb)

Additional file 10: Video S2b. 3D reconstruction of a live 1wk-old anesthetized male CPB adult. MPR rendering of a live 1wk-old anesthetized adult male Colorado potato beetle (*L. decemlineata*) showing the arrangement of in situ internal structures supported by the exoskeleton at 20 μm isotropic voxel spacing (micro-CT data acquired using Protocol 3). (MOV 711 kb)

Additional file 11: Video S3a. 3D reconstruction of a live 1d-old anesthetized female TAW adult. Volume rendering of a live 1d-old (sexually immature) anesthetized adult female true armyworm (*P. unipuncta*) showing the exoskeleton, soft tissues, and tracheal system at 20 μm isotropic voxel spacing (micro-CT data acquired using Protocol 3). (MOV 2574 kb)

Additional file 12: Video S3b. 3D reconstruction of a live 1d-old anesthetized female TAW adult. MPR rendering of a live 1d-old (sexually immature) anesthetized adult female true armyworm (*P. unipuncta*) showing the arrangement of in situ internal structures supported by the exoskeleton at 20 μm isotropic voxel spacing (micro-CT data acquired using Protocol 3). (MOV 877 kb)

Additional file 13: Video S4a. 3D reconstruction of a live 4d-old anesthetized female TAW adult. Volume rendering of live 4d-old (sexually mature) anesthetized adult female true armyworm (*P. unipuncta*) demonstrating the exoskeleton, soft tissues, and tracheal system at 20 μm isotropic voxel spacing (micro-CT data acquired using Protocol 3). (MOV 2574 kb)

Additional file 14: Video S4b. 3D reconstruction of a live 4d-old anesthetized female TAW adult. MPR rendering of a live 4d-old (sexually mature) anesthetized adult female true armyworm (*P. unipuncta*) illustrating the arrangement of in situ internal structures supported by the exoskeleton at 20 μm isotropic voxel spacing (micro-CT data acquired using Protocol 3). (MOV 1308 kb)

Additional file 15: Video S5a. 3D reconstruction of a live 1d-old anesthetized male TAW adult. Volume rendering of a live 1d-old (sexually immature) anesthetized adult male true armyworm (*P. unipuncta*) showing the exoskeleton, soft tissues, and tracheal system at 20 μm isotropic voxel spacing (micro-CT data acquired using Protocol 3). (MOV 2565 kb)

Additional file 16: Video S5b. 3D reconstruction of a live 1d-old anesthetized male TAW adult. MPR rendering of a live 1d-old (sexually immature) anesthetized adult male true armyworm (*P. unipuncta*) demonstrating the arrangement of in situ internal structures supported

by the exoskeleton at 20 μm isotropic voxel spacing (micro-CT data acquired using Protocol 3). (MOV 816 kb)

Additional file 17: Video S6a. 3D reconstruction of a live 4d-old anesthetized male TAW adult. Volume rendering of live 4d-old (sexually mature) anesthetized adult male true armyworm (*P. unipuncta*) illustrating the exoskeleton, soft tissues, and tracheal system at 20 μm isotropic voxel spacing (micro-CT data acquired using Protocol 3). (MOV 2518 kb)

Additional file 18: Video S6b. 3D reconstruction of a live 4d-old anesthetized male TAW adult. MPR rendering of a live 4d-old (sexually mature) anesthetized adult male true armyworm (*P. unipuncta*) showing the arrangement of in situ internal structures supported by the exoskeleton at 20 μm isotropic voxel spacing (micro-CT data acquired using Protocol 3). (MOV 658 kb)

Abbreviations

ANOVA: Analysis of variance; ATP: Adenosine triphosphate; CNS: Central nervous system; CO₂: Carbon dioxide; CPB: Colorado potato beetle; F: Female; IM: Sexually immature; KMO: Kaiser-Meyer-Olkin; M: Male; MAT: Sexually mature; micro-CT: Micro-computed tomography; MPR: Multi-planar reformatted; NMJ: Neuromuscular junction; OA: Orthogonal array; PCA: Principal component analysis; R: Repeated exposure; ROI: Regions of interest; S: Single exposure; S/N: Signal-to-noise; TAW: True armyworm

Acknowledgements

We thank I. Scott (Agriculture and Agri-Food Canada, London, Ontario) for providing the CPB adults.

Funding

Research funding was provided by the Natural Sciences and Engineering Research Council of Canada (Grants 04294 and 9551 to D.W.H and J.N.M, respectively).

Availability of data and materials

Data acquired and materials used for this study are kept at the Preclinical Imaging Research Centre, Robarts Research Institute, Schulich School of Medicine and Dentistry, Western University. Datasets acquired and/or analysed during the current study can be made available from the corresponding author on reasonable request.

Authors' contributions

DP, JKK, and DWH conceived the imaging method; DP, JKK, and JNM conceived the insect life history study; DP and JKK designed the set up, tested the anesthetic method, scanned the live insects, performed the OA experiments, and analysed the data; DP performed the image analysis; JUU and DP performed the noise quantification and analysis; CJDN and DP performed the dosimetry measurements and analysis. All authors discussed, commented, and contributed to writing the manuscript. All authors read and approved the final manuscript.

Ethics approval and consent to participate

Not applicable.

Consent for publication

Not applicable.

Competing interests

The authors declare that they have no competing interests.

Publisher's Note

Springer Nature remains neutral with regard to jurisdictional claims in published maps and institutional.

Author details

¹Preclinical Imaging Research Centre, Robarts Research Institute, Schulich School of Medicine and Dentistry, Western University, London, ON, Canada. ²Department of Biology, Western University, London, ON, Canada. ³London Research and Development Centre, Agriculture and Agri-Food Canada, London, ON, Canada.

Received: 3 March 2017 Accepted: 10 July 2017

Published online: 31 July 2017

References

- Friedrich F, Matsumura Y, Pohl H, Bai M, Hörschemeyer T, Beutel RG. Insect morphology in the age of phylogenomics: innovative techniques and its future role in systematics. *Entomol Sci.* 2014;17:1–24.
- Holdsworth DW, Thornton MM. Micro-CT in small animal and specimen imaging. *Trends Biotechnol.* 2002;20:534–9.
- Bartling S, Stiller W, Semmler W. Small animal computed tomography imaging. *Curr Med Imaging Rev.* 2007;3:45–59.
- Hart AG, Bowtell RW, Köckenberger W, Wenseleers T, Ratnieks FLW. Magnetic resonance imaging in entomology: a critical review. *J Insect Sci.* 2003;3:5.
- Betz O, Wegst U, Weide D, Heethoff M, Helfen L, Lee W-K, et al. Imaging applications of synchrotron X-ray phase-contrast microtomography in biological morphology and biomaterials science. I. General aspects of the technique and its advantages in the analysis of millimetre-sized arthropod structure. *J Microsc.* 2007;227:51–71.
- Socha JJ, Westneat MW, Harrison JF, Waters JS, Lee W-K. Real-time phase-contrast x-ray imaging: a new technique for the study of animal form and function. *BMC Biol.* 2007;5:6.
- Sena G, Almeida AP, Braz D, Nogueira LP, Soares J, Azambuja P, et al. On the possibilities of polychromatic synchrotron radiation microtomography for visualization of internal structures of *Rhodnius prolixus*. *Radiat Phys Chem.* 2015;115:179–82.
- Sombke A, Lipke E, Michalik P, Uhl G, Harzsch S. Potential and limitations of X-ray micro-computed tomography in arthropod neuroanatomy: a methodological and comparative survey. *J Comp Neurol.* 2015;523:1281–95.
- Westneat M, Socha J, Lee W. Advances in biological structure, function, and physiology using synchrotron X-ray imaging. *Annu Rev Physiol.* 2008;70:119–42.
- Socha J, De Carlo F. Use of synchrotron tomography to image naturalistic anatomy in insects. *Proc SPIE.* 2008;7078:A–1.
- Hörschemeyer T, Beutel RG, Pasop F. Head structures of *Priacma serrata leconte* (Coleoptera: Archostemata) inferred from X-ray tomography. *J Morphol.* 2002;252:298–314.
- Westneat MW, Betz O, Blob RW, Fezzaa K, Cooper WJ, Lee W-K. Tracheal respiration in insects visualized with synchrotron x-ray imaging. *Science (80-).* 2003;299:558–60.
- Dinley J, Hawkins L, Paterson G, Ball AD, Sinclair I, Sennett-Jones P, et al. Micro-computed X-ray tomography: a new non-destructive method of assessing sectional, fly-through and 3D imaging of a soft-bodied marine worm. *J Microsc.* 2010;238:123–33.
- Greco M, Bell D, Woolnough L, Laycock S, Corps N, Mortimore D, et al. 3-D visualisation, printing, and volume determination of the tracheal respiratory system in the adult desert locust, *Schistocerca gregaria*. *Entomol Exp Appl.* 2014;152:42–51.
- Iwan D, Kamiński MJ, Raś M. The last breath: a μCT -based method for investigating the tracheal system in Hexapoda. *Arthropod Struct Dev.* 2015; 44:218–27.
- Postnov A, De Clerck N, Sasov A, Van Dyck D. 3D in-vivo X-ray microtomography of living snails. *J Microsc.* 2002;205:201–4.
- Nahirney PC, Forbes JG, Morris HD, Chock SC, Wang K. What the buzz was all about: superfast song muscles rattle the tymbals of male periodical cicadas. *FASEB J.* 2006;20:2017–26.
- Metscher B. MicroCT for comparative morphology: simple staining methods allow high-contrast 3D imaging of diverse non-mineralized animal tissues. *BMC Physiol.* 2009;9:11.
- Lowe T, Garwood RJ, Simonsen TJ, Bradley RS, Withers PJ. Metamorphosis revealed: time-lapse three-dimensional imaging inside a living chrysalis. *J R Soc Interface.* 2013;10:20130304.
- Greco MK, Tong J, Soleimani M, Bell D, Schäfer MO. Imaging live bee brains using minimally-invasive diagnostic radioentomology. *J Insect Sci.* 2012;12:89.
- dos Santos RT, Ershov A, van de Kamp T, Baumbach T. In vivo X-ray cine-tomography for tracking morphological dynamics. *Proc Natl Acad Sci.* 2014; 111:3921–6.
- Mokso R, Schwyn DA, Walker SM, Doube M, Wicklein M, Müller T, et al. Four-dimensional in vivo X-ray microscopy with projection-guided gating. *Sci Rep.* 2015;5:8727.

23. Chandna S, Dwarakanath BS, Seth RK, Khaitan D, Adhikari JS, Jain V. Radiation responses of Sf9, a highly radioresistant lepidopteran insect cell line. *Int J Radiat Biol.* 2004;80:301–15.
24. Bakri A, Mehta K, Lance DR. Sterilizing insects with ionizing radiation. In: Dyck VA, Hendrichs J, Robinson AS, editors. *Sterile insect tech.* Berlin: Springer-Verlag; 2005. p. 233–68.
25. Cheng I-C, Lee H-J, Wang TC. Multiple factors conferring high radioresistance in insect Sf9 cells. *Mutagenesis.* 2009;24:259–69.
26. Koval TM. Intrinsic resistance to the lethal effects of x-irradiation in insect and arachnid cells. *Proc Natl Acad Sci U S A National Acad Sciences.* 1983;80:4752–5.
27. Nicolas G, Sillans D. Immediate and latent effects of carbon dioxide on insects. *Annu Rev Entomol.* 1989;34:97–116.
28. Badre NH, Martin ME, Cooper RL. The physiological and behavioral effects of carbon dioxide on *Drosophila melanogaster* larvae. *Comp Biochem Physiol Part A.* 2005;140:363–76.
29. Bierbower SM, Cooper RL. The mechanistic action of carbon dioxide on a neural circuit and NMJ communication. *J Exp Zool Part A.* 2013;319:340–54.
30. Wegener G. Hypoxia and posthypoxic recovery in insects: physiological and metabolic aspects. In: Hochachka PW, Lutz PL, Sick TJ, Rosenthal M, editors. *Surviv. Hypoxia Mech. Control adapt.* Boca Raton: CRC Press Inc.; 1993. p. 417–34.
31. Perron JM, Huot L, Corriveau G-W, Chawla SS. Effects of carbon dioxide anaesthesia on *Drosophila melanogaster*. *J Insect Physiol.* 1972;18:1869–74.
32. Tanaka A. Effects of carbon-dioxide anaesthesia on the number of instars, larval duration and adult body size of the German cockroach, *Blattella germanica*. *J Insect Physiol.* 1982;28:813–21.
33. Barron AB. Anaesthetising drosophila for behavioural studies. *J Insect Physiol.* 2000;46:439–42.
34. Branscome DD, Koehler PG, Oi FM. Influence of carbon dioxide gas on German cockroach (Dictyoptera: Blattellidae) knockdown, recovery, movement and feeding. *Physiol Entomol.* 2005;30:144–50.
35. Nilson TL, Sinclair BJ, Roberts SP. The effects of carbon dioxide anaesthesia and anoxia on rapid cold-hardening and chill coma recovery in *Drosophila melanogaster*. *J Insect Physiol.* 2006;52:1027–33.
36. Cobb BD, Clarkson JM. A simple procedure for optimising the polymerase chain reaction (PCR) using modified Taguchi methods. *Nucleic Acids Res.* 1994;22:3801–5.
37. Rao RS, Kumar CG, Prakasham RS, Hobbs PJ. The Taguchi methodology as a statistical tool for biotechnological applications: a critical appraisal. *Biotechnol J.* 2008;3:510–23.
38. Poinapen D, Brown DCW, Beeharry GK. Seed orientation and magnetic field strength have more influence on tomato seed performance than relative humidity and duration of exposure to non-uniform static magnetic fields. *J Plant Physiol.* 2013;170:1251–8.
39. Taguchi G. Introduction to quality engineering: designing quality into products and processes, Asian productivity organization; 1986.
40. Taguchi G. System of experimental design; engineering methods to optimize quality and minimize costs. New York: UNIPUB/Kraus International; 1987.
41. Willis ER, Roth LM. A microscope stage for continuous anaesthesia of insects. *Science.* 1949;109:230.
42. Colinet H, Renault D. Metabolic effects of CO₂ anaesthesia in *Drosophila melanogaster*. *Biol Lett.* 2012;8:1050–4.
43. Ford NL, Thornton MM, Holdsworth DW. Fundamental image quality limits for microcomputed tomography in small animals. *Med Phys.* 2003;30:2869–77.
44. Feldkamp LA, Davis LC, Kress JW. Practical cone-beam algorithm. *J Opt Soc Am A.* 1984;1:612.
45. Hedayat AS, Sloane NJA, Stufken J. Orthogonal arrays: theory and applications. New York: Springer-Verlag; 1999.
46. Fields A. Discovering statistics using SPSS. 3rd ed. London: SAGE Publication Ltd.; 2009.
47. Cheeseman JF, Winnebeck EC, Millar CD, Kirkland LS, Sleight J, Goodwin M, et al. General anaesthesia alters time perception by phase shifting the circadian clock. *Proc Natl Acad Sci.* 2012;109:7061–6.
48. Bartholomew NR, Burdett JM, VandenBrooks JM, Quinlan MC, Call GB. Impaired climbing and flight behaviour in *Drosophila melanogaster* following carbon dioxide anaesthesia. *Sci Rep.* 2015;5:15298.
49. Lighton JRB, Schilman PE. Oxygen reperfusion damage in an insect. Hermes-lima M, editor. *PLoS One.* 2007;2:e1267.
50. Wegener G. Insect brain metabolism under normoxic and hypoxic conditions. In: Gupta AP, editor. *Arthropod Brain Ints Evol. Dev. Struct. Funct.* New York: John Wiley & Sons; 1987. p. 369.
51. Slansky FJ. Food consumption and utilization. In: Kerkut G.A., L.I. G, editors. *Compr. Insect Physiol. Biochem. Pharmacol.* Vol 4. Oxford: Pergamon Press; 1985. p. 87–163.
52. Socha JJ, Förster TD, Greenlee KJ. Issues of convection in insect respiration: insights from synchrotron X-ray imaging and beyond. *Respir Physiol Neurobiol.* 2010;173:565–73.
53. Mastrangelo T, Parker AG, Jessup A, Pereira R, Orozco-Dávila D, Islam A, et al. A new generation of X ray irradiators for insect sterilization. *J Econ Entomol.* 2010;103:85–94.
54. South A, Lewis SM. The influence of male ejaculate quantity on female fitness: a meta-analysis. *Biol Rev.* 2011;86:299–309.

Submit your next manuscript to BioMed Central and we will help you at every step:

- We accept pre-submission inquiries
- Our selector tool helps you to find the most relevant journal
- We provide round the clock customer support
- Convenient online submission
- Thorough peer review
- Inclusion in PubMed and all major indexing services
- Maximum visibility for your research

Submit your manuscript at
www.biomedcentral.com/submit

